© 1999 Oxford University Press
Nucleic Acids Research, 1999, Vol. 27, No. 4 **1063–1069**

The salt dependence of DNA recognition by NF-κB p50: a detailed kinetic analysis of the effects on affinity and specificity

Darren J. Hart, Robert E. Speight, Matthew A. Cooper[1], John D. Sutherland[2] and Jonathan M. Blackburn*

Department of Biochemistry, University of Cambridge, Tennis Court Road, Cambridge CB2 1QW, UK,
[1]Department of Chemistry, University of Cambridge, Lensfield Road, Cambridge CB1 2EW, UK and
[2]Department of Chemistry, University of Manchester, Oxford Road, Manchester M13 9PL, UK

Received October 9, 1998; Revised and Accepted January 4, 1999

ABSTRACT

The binding kinetics of NF-κB p50 to the Ig-κB site and to a DNA duplex with no specific binding site were determined under varying conditions of potassium chloride concentration using a surface plasmon resonance biosensor. Association and dissociation rate constants were measured enabling calculation of the dissociation constants. Under previously established high affinity buffer conditions, the k_a for both sequences was in the order of 10^7 $M^{-1}s^{-1}$ whilst the k_d values varied 600-fold in a sequence-dependent manner between 10^{-1} and 10^{-4} s^{-1}, suggesting that the selectivity of p50 for different sequences is mediated primarily through sequence-dependent dissociation rates. The calculated K_D value for the Ig-κB sequence was 16 pM, whilst the K_D for the non-specific sequence was 9.9 nM. As the ionic strength increased to levels which are closer to that of the cellular environment, the binding of p50 to the non-specific sequence was abolished whilst the specific affinity dropped to nanomolar levels. From these results, a mechanism is proposed in which p50 binds specific sequences with high affinity whilst binding non-specific sequences weakly enough to allow efficient searching of the DNA.

INTRODUCTION

The mammalian DNA-binding protein NF-κB p50 is a member of a family of eukaryotic transcription factors that contain a 300 amino acid region of high homology to the *rel* oncogene product (1). The Rel homology region contains DNA-binding, dimerisation and nuclear localisation functions. NF-κB p50 is synthesised as a 105 kDa precursor protein which is proteolytically cleaved to yield the mature transcription factor (2). Dimerisation may occur between two p50 monomers, or between p50 and other members of the family (e.g. p65; 3–5) which may also possess C-terminal transactivation domains.

Dimeric Rel proteins are sequestered in the cytoplasm, remote from their site of action in the nucleus, by association with proteins of the IκB family which are thought to mask a nuclear localisation signal (6). NF-κB inducers such as phorbol esters, lipopolysaccharide, ultraviolet light, inflammatory cytokines and bacterial and viral pathogens activate signal transduction pathways leading to phosphorylation and ubiquitination of IκB (1,7). Consequent proteasome-mediated IκB proteolysis results in translocation of dimeric transcription factors to the nucleus where they regulate transcription of a wide variety of genes. These are involved in processes such as immune functions, antiviral and antimicrobial responses, inflammation, apoptosis and even processes as fundamental as limb development (1,8–10).

The specificity of NF-κB for DNA is due in part to homodimeric and heterodimeric permutations of monomeric subunits binding with different affinities to a range of binding sites (11), thereby conferring varying transcriptional activities. NF-κB binds regulatory elements of the promoter and up- or down-regulates transcription through synergistic or antagonistic DNA–protein and protein–protein interactions with other transcription factors. These can be sequence-specific factors such as the zinc finger protein Sp1 (12), or the basal transcription factors of the preinitiation complex such as TBP and TFIIB which bind the transactivation domain of NF-κB p65 (13). Since p50 homodimer has no such domain, it is assumed to repress transcription by competition for binding sites (14) unless nuclear cofactors, e.g. Bcl-3, are present to form a transcription-activating ternary complex (12). Co-operative binding of NF-κB with high mobility group (HMG) proteins to the same DNA sequence has been demonstrated as a prerequisite for transcription from some promoters and is thought to be a result of architectural changes in the DNA (15–17).

The X-ray crystallographic structures of protein–DNA complexes have been solved for homodimers of p50 (18,19), p52 (20) and p65 (21), and the p50/p65 heterodimer (4). These show the NF-κB monomer to consist of two immunoglobulin-like domains joined by a flexible loop. The N-terminal domain contributes the majority of the protein–DNA contacts whilst the C-terminal domain mediates dimerisation through a C2 symmetrical interaction of interdigitating hydrophobic residues projecting from the face of a β-sheet. Since no structure is available for free dimer, a comparison with the DNA-bound protein to assess changes upon binding has not been possible. However, conformational change of both DNA-binding domain and DNA upon formation of a protein–DNA complex has been inferred by circular dichroism (CD) spectroscopy and changes in protease sensitivity (22). The crystal structures of p50 and p65

*To whom correspondence should be addressed. Tel: +44 1223 766044; Fax: +44 1223 766002; Email: jmb50@cam.ac.uk

dimerisation domains have been solved (5) and reveal no change in structure of this domain upon DNA-binding. The p50 structures reveal that there are a high number of phosphate backbone contacts by basic residues of the DNA-contacting loops (18,19). Twelve of the 18 phosphates of the target site are contacted by the protein with a total of 18 phosphate contacts per DNA–dimer complex (18). Therefore, it is possible that the initial recognition event is between p50 and the negatively charged phosphate backbone of the DNA, with the DNA-binding domains assuming a tighter binding form upon specific sequence recognition.

Previous kinetic studies of NF-κB/DNA interaction using electrophoretic mobility shift assays (EMSA) have identified high affinity Rel dimer–DNA interactions (11,23) and have shown that the protein binds to specific DNA sequences with an apparent K_D in the order of 10^{-12} M. However, absolute values for K_D are often found to be buffer-dependent, and the physiological significance of such high affinities achieved in optimised buffers is unclear. Binding constants are usually determined when the binding reaction is at equilibrium, and individual association and dissociation rate constants are rarely determined with any accuracy.

Extensive studies on the binding of the *lac* repressor to DNA have demonstrated the sensitivity of that system to salt concentration *in vitro* (24–26). However there is still a considerable degree of uncertainty in the finer details of this protein–DNA interaction, for example the relative roles of tetramerisation, interstrand transfer, wrapping and looping of DNA and sliding in DNA recognition (27–29). As such, it is not yet clear whether the *lac* repressor data will prove to be generally applicable to other DNA-binding proteins or not (27).

The present study concerns the eukaryotic transcription factor NF-κB p50 which is known to differ in several respects from the prokaryotic *lac* repressor. For example, the *lac* repressor is a tetramer utilising classic helix–turn–helix motifs in DNA recognition, whereas the p50 homodimer wraps itself around two thirds of the cylindrical surface of the double helix leaving only the minor groove free. In addition, the functional requirements of a bacterial repressor protein and a eukaryotic transactivator might be expected to result in significantly different binding kinetics, both through their relative needs to compete for DNA binding with other proteins and because the high degree of packaging of eukaryotic DNA might preclude extensive sliding as a mechanism of sequence searching. It does not therefore seem reasonable a priori to extrapolate directly from the kinetic and thermodynamic analyses of the *lac* repressor–DNA interaction to the p50–DNA interaction. However, a detailed understanding of the nature of the NF-κB–DNA interaction is of increasing significance given the importance of this transcription factor as a therapeutic target (30,31). To this end we report here the use of a surface plasmon resonance (SPR) optical biosensor to characterise the association and dissociation kinetics of binding of NF-κB p50 to specific and non-specific DNA in buffer conditions of varying salt concentration. We also speculate on the physiological significance of the data generated.

MATERIALS AND METHODS

NF-κB p50 homodimer

The active fragment of p50 consisting of amino acids 40–366 (19) was expressed in *Escherichia coli* BL21 (DE3) from the T7-based transcription vector pLM1-p50 (32). A 5 ml saturated overnight culture of BL21(DE3) [pLM1p50] in 2× TY (ampicillin 50 μg/ml) was used as the inoculum for a 500 ml culture which was incubated at 37°C, 200 r.p.m. until an optical density of 0.4 was reached. IPTG was added to a final concentration of 100 μM and the culture was further incubated for 12 h. Cells were harvested by centrifugation and the pellet resuspended in 25 ml of lysis buffer (50 mM Tris–HCl pH 7.4, 5 mM DTT, 1 mM EDTA, 100 mM NaCl) supplemented with hen egg white lysozyme (Sigma) at 0.2 mg/ml. After 2 h at room temperature, further lysis and shearing of genomic DNA was achieved by sonication. The lysate was then cleared by centrifugation and quantitated at 10 mg/ml by Bradford assay. DNA was precipitated by addition of polyethylene imine (0.5% v/v) to 15 ml of the lysate which was placed on ice for 15 min and then centrifuged. The supernatant was recovered and 30 ml of saturated ammonium sulphate solution was added to precipitate p50 which was then pelleted by centrifugation. The pellet was resuspended in 20 mM HEPES, 2 mM EDTA, 1 mM DTT, 5% (v/v) glycerol pH 7.4 and the p50 purified by FPLC on a Mono S HR16/10 cation exchange column (Pharmacia) with a 0–1 M NaCl gradient. The p50 eluted at ~400 mM NaCl. Protein purity was assessed by SDS–PAGE with Coomassie Blue staining and the concentration was determined to be 0.6 mg/ml using an accurate spectrophotometric method (33) with an extinction coefficient of 19 791 $mol^{-1}cm^{-1}$ for native p50.

Duplex DNA

Two duplex DNA molecules containing an Ig-κB p50 binding site and a non-binding control sequence were generated by annealing complementary oligonucleotides of 30 bases in length, one of which was 5′-biotinylated during synthesis. Annealing was performed with biotinylated and unbiotinylated oligonucleotides at concentrations of 5 and 6 μM respectively in 10 mM Tris–HCl pH 7.4, 1 mM EDTA, 100 mM NaCl by cooling from 95 to 35°C over 30 min. The sequences of the oligonucleotides used in the construction of the Ig-κB duplex were 5′-biotin-AGCTT CAGAG GGGAC TTTCC GAGAG TACTG-3′ and the complementary 5′-GATCC AGTAC TCTCG GAAAG TCCCC TCTGA-3′. The underlined region is the p50 binding site and in the biotinylated strand of the non-specific control was ATCGA TCGGA.

SPR

The SPR instrument was a BIAcore 2000 optical biosensor (BIAcore AB). Kinetic analyses of sensorgrams were performed using BIAeval 3.0 global analysis software based on algorithms for numerical integration (34), and manually using spreadsheet and graphing software. A commercially available SA sensor chip (BIAcore AB) was used which consisted of a thin gold film coated with a carboxymethyldextran hydrogel matrix to which streptavidin was cross-linked. The running buffer used for DNA immobilisation and SPR assay was 10 mM Tris–HCl pH 7.4, 0.2 mM EDTA, 3 mM DTT, 0.02% Triton X-100, 10% glycerol and KCl at 75–150 mM. This buffer was similar to that used in a previous EMSA analysis of p50 (35). The buffer was freshly prepared, filtered through a 0.22 μm membrane and degassed prior to use.

DNA immobilisation

The biotinylated DNA duplexes at 500 pM were injected at a flow rate of 10 μl/min across individual flowcells of the sensor chip until

20 response units (RU) had been immobilised. One response unit corresponds to a surface density of DNA of ~1 pg/mm^2 (36). One flowcell was left underivatised to control for non-specific protein binding to the sensor chip matrix, bulk refractive index changes between the injected solution and the running buffer and baseline drift. After use, the sensor chip was washed in deionised water, dried and stored over dry silica gel at 4°C. Reproducible levels of protein binding were maintained for at least three sets of experiments.

SPR assay

Purified p50 was diluted to nanomolar concentrations in running buffer and injected for 360 s at a flow rate of 20 µl/min over DNA-derivatised and control flowcells. The protein sample was then replaced by running buffer at the same flow rate and the protein–DNA complex allowed to dissociate for 1200 s. The chip surface was regenerated with an injection of buffer supplemented with 2 M NaCl for 10 s. All assays were carried out at 25°C.

SPR data analysis

Data were prepared for kinetic analysis by aligning sensorgrams such that the points of injection were superimposed. The sensorgram from the underivatised flow cell was subtracted from those with DNA to correct for signal drift and bulk refractive index changes. The process being observed can be described by the equation:

$$[\text{DNA}] + [\text{Protein}] \underset{k_d}{\overset{k_a}{\rightleftharpoons}} [\text{Protein–DNA complex}] \qquad \mathbf{1}$$

Upon injection through the SPR flow cell, the protein solution is replenished within the system so the protein concentration effectively remains constant at the initial value C. The total amount of DNA ligand present is expressed in terms of R_{max}, the maximum possible response and the amount of complex formed is proportional to R, the observed response. Thus, after time t the concentration of analyte is C and the amount of free DNA is given by $R_{max} - R$. The rate of formation of the protein–DNA complex (dR/dt) can therefore be expressed in the form of equation **2** which can be rearranged to **3**.

$$dR/dt = k_aC(R_{max} - R) - k_dR \qquad \mathbf{2}$$

$$dR/dt = k_aCR_{max} - (k_aC + k_d)R \qquad \mathbf{3}$$

Sensorgrams were recorded for four protein concentrations ranging from 2.5 to 20 nM and dR/dt against R was plotted for each concentration. The gradient of each of these lines ($k_aC + k_d$) represents the observed association rate, $-k_{obs}$. A plot of $-k_{obs}$ against C allows k_a to be determined from equation **4**.

$$-k_{obs} = k_aC + k_d \qquad \mathbf{4}$$

At the end of the sample injection, the protein solution was replaced by running buffer and the bound protein dissociated from the immobilised DNA. Since the concentration of protein in the running buffer was zero, and assuming negligible rebinding, equation **2** simplifies to **5**.

$$dR/dt = -k_dR \qquad \mathbf{5}$$

$$\ln (R_0/R_1) = k_d(t_1 - t_0) \qquad \mathbf{6}$$

Integrating **5** leads to equation **6** which shows that a plot of ln (R_0/R_1) against ($t_1 - t_0$) has a gradient k_d. The dissociation constant (K_D) can be obtained from the ratio of the rate constants **7**.

$$K_D = k_d/k_a \qquad \mathbf{7}$$

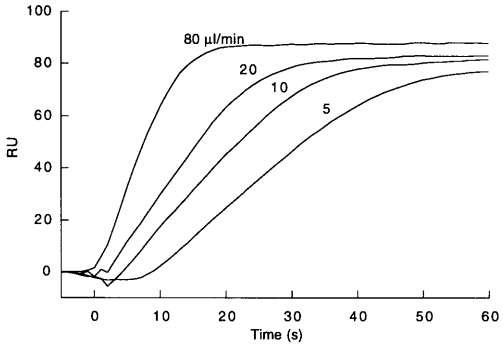

Figure 1. The effect of varying flow rate upon the observed association rate of p50 (20 nM) with 20 RU of Ig-κB-specific DNA.

An alternative method for determining K_D is by Scatchard analysis of the equilibrium binding values (R_{eq}) for different protein concentrations. This is only possible if the association phase is long enough for the binding reaction to reach equilibrium. Since the net rate of binding at equilibrium is zero, equation **3** can be rearranged to **8**.

$$R_{eq}/C = (R_{max}/K_D) - (R_{eq}/K_D) \qquad \mathbf{8}$$

Therefore, a plot of R_{eq}/C against R_{eq} has a gradient of $-1/K_D$.

RESULTS

Mass transport-limited binding

The effects of mass transport upon binding were examined by comparing the observed association rates at varying flow rate. The rate of association was shown to increase with increasing flow rate (Fig. 1) which is a characteristic of mass transport-limited binding (37). This occurs when the binding of the analyte to ligand is faster than the diffusion of the analyte from the bulk solution to the ligand at the surface. This also results in increased rebinding of the analyte in the dissociation phase, as the released analyte can rebind to free ligand before removal into bulk solution. To minimise these effects, very low levels (20 RU) of DNA were immobilised and a high flow rate was employed (38). Optimisation of these experimental conditions increased the region of association and dissociation data that could be used in the kinetic analysis of p50 binding.

Binding to specific and non-specific DNA

A buffer in which p50 binds to specific DNA with picomolar affinity (35) formed the basis of the running buffer for the SPR assays and contains KCl at 100 mM. The KCl component of this buffer was also adjusted to 75, 125 and 150 mM to investigate the effect of salt concentration on p50 binding. Sensorgrams for the binding of a range of concentrations of p50 to immobilised Ig-κB-specific DNA and non-specific DNA were obtained (Figs 2 and 3).

This data set was fitted globally to a model describing mass transport-limited binding of an analyte to ligand using algorithms supplied with the BIAeval 3.0 analysis package (38). Global fitting of the data shown in Figure 2a–d gave $k_a = 1.5 \times 10^7$ M^{-1}s^{-1}, $k_d = 1.3 \times 10^{-4}$s^{-1}, and an affinity of 8.6 pM (overall $\chi^2 = 4.2$). From visual inspection of the global fit, however, it was apparent that the fitted dissociation rate was faster than the observed dissociation rate.

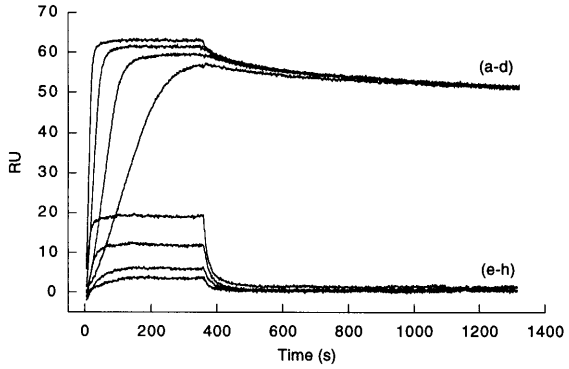

Figure 2. Sensorgrams of 20, 10, 5 and 2.5 nM NF-κB p50 binding to 20 RU of immobilised Ig-κB-specific DNA (a–d) and non-specific DNA (e–h) in running buffer containing 100 mM KCl. The upper curve of each series corresponds to the highest concentration of p50.

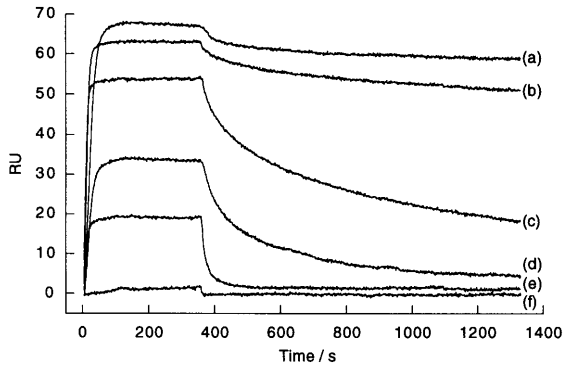

Figure 3. Sensorgrams of 20 nM NF-κB p50 binding in 75 mM (a and d), 100 mM (b and e) and 125 mM (c and f) KCl buffer to Ig-κB-specific DNA (a–c) and non-specific DNA (d–f). Data for 150 mM KCl buffer are omitted for clarity.

For this reason, the association and dissociation phases of the binding curve were analysed separately using manual methods.

The association rate constants for binding to specific and non-specific DNA at both 75 and 100 mM KCl were almost identical (Fig. 4; Table 1). At 125 and 150 mM, no binding to non-specific DNA was observed, so values for k_a could not be obtained. The association rates increased slightly with increasing salt concentration (Table 1).

The non-linearity of the dissociation plot for non-specific DNA (Fig. 5a) was probably a consequence of mass transport-limited rebinding of dissociated p50, since the rate of dissociation decreased as the extent of dissociation increased (i.e. more sites became available). Since this effect would be minimal during the initial period of dissociation when the density of free DNA was low, the value of k_d was calculated from the initial 10 s of the dissociation phase of the sensorgram for the highest concentration of p50 (Table 1). In contrast, the dissociation plots for Ig-κB suggested a biphasic process whereby a short period of rapid dissociation of a small amount of material gave way to a longer period of slow dissociation (Fig. 5b). This type of phenomenon has been observed previously in DNA–protein interactions and was attributed to heterogeneity in immobilised DNA or protein (39). Here it can perhaps be accounted for by dissociation of p50

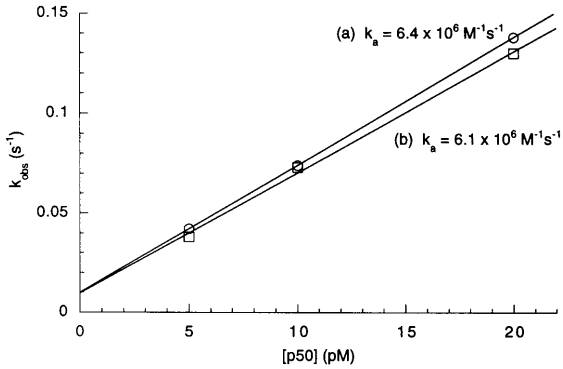

Figure 4. Plots of $-k_{obs}$ against C for the association data of NF-κB p50 binding to 20 RU of immobilised Ig-κB-specific DNA (a) and non-specific DNA (b) in running buffer containing 100 mM KCl. The gradient of the line is k_a.

from the regions of the DNA duplex flanking the binding site masking the true dissociation rate for specifically-bound p50. The k_d for specifically-bound p50 was determined from the later phase (500–1000 s after the start of dissociation) once the initial faster dissociation had diminished. In this specific dissociation period, the surface of the flowcell remains almost fully saturated with specifically bound protein due to the slow rate of dissociation, thus rebinding in this phase would be expected to be minimal. The values of k_d for p50 dissociation from Ig-κB and non-specific DNA are shown in Table 1.

Table 1. Kinetic constants (k_a and k_d) and calculated and measured dissociation constants (K_D) for binding of p50 to Ig-κB and non-specific DNA

		Rate constant		K_D (M)	
[KCl] (mM)	DNA	k_a ($M^{-1}s^{-1}$)	k_d (s^{-1})	k_d/k_a	Scatchard
75	Ig-κB	3.3×10^6	4.1×10^{-5}	1.3×10^{-11}	1.6×10^{-9}
	non-specific	3.3×10^6	1.1×10^{-2}	3.3×10^{-9}	7.7×10^{-9}
100	Ig-κB	6.4×10^6	1.0×10^{-4}	1.6×10^{-11}	3.2×10^{-10}
	non-specific	6.1×10^6	6.0×10^{-2}	9.9×10^{-9}	3.8×10^{-8}
125	Ig-κB	8.4×10^6	6.6×10^{-4}	7.8×10^{-11}	6.6×10^{-10}
	non-specific	No binding observed		-	-
150	Ig-κB	1.1×10^7	5.9×10^{-3}	5.3×10^{-10}	2.3×10^{-9}
	non-specific	No binding observed		-	-

The dissociation rates for both non-specific DNA and Ig-κB increased with KCl concentration, but to different degrees. The rates of dissociation of p50 from non-specific DNA relative to those from Ig-κB were 268-fold higher in 75 mM KCl and 600-fold higher in 100 mM KCl. This ratio could not be determined in 125 and 150 mM KCl buffers, as no binding of p50 to non-specific DNA was observed. However, the similarity in association data obtained for specific and non-specific sequences at 75 and 100 mM KCl, and also from a comparison of different specific sequences in 100 mM KCl buffer (data not shown), suggests that the association rate would be equal to that observed with Ig-κB. The absence of apparent binding is most likely a result of salt-induced high dissociation rates preventing accumulation of protein on the DNA to a detectable level.

The measurement of both k_a and k_d allows K_D to be calculated (equation **7**) (Table 1). Whilst K_D values for binding to Ig-κB in

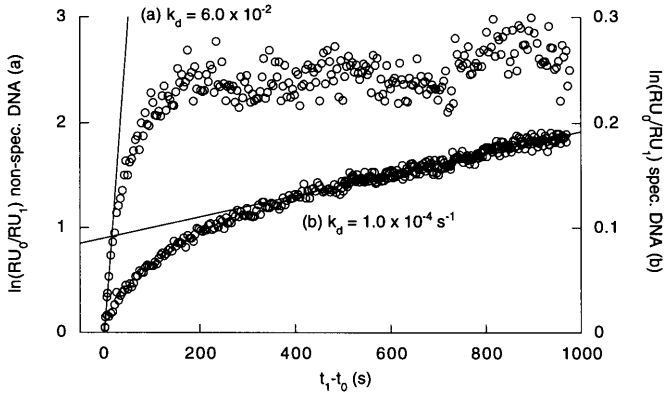

Figure 5. Plots of $ln(R_0/R_1)$ against $(t_1 - t_0)$ for the dissociation of 20 nM NF-κB p50 from non-specific DNA (a) and Ig-κB-specific DNA (b) in running buffer containing 100 mM KCl. Each fourth data point is shown.

75 and 100 mM KCl buffer were similar (13 and 16 pM), the protein both associated and dissociated more rapidly in the latter. The affinity of p50 for non-specific DNA was much lower than for Ig-κB, and this was entirely manifested in the different dissociation rates. The calculated values of K_D for binding of p50 to non-specific DNA in 75 and 100 mM KCl buffer were 3.3 and 9.9 nM respectively, which showed that non-specific binding was reduced at higher salt concentrations. Again, the lower affinity at the higher salt concentration was despite an ~2-fold increase in association rate and due to the higher dissociation rate. It was not possible to calculate a K_D for non-specific DNA at 125 and 150 mM KCl, but presumably it is very high in comparison to Ig-κB.

Scatchard analysis of equilibrium binding values permitted a direct measurement of K_D in a manner analogous to EMSA analysis. The K_D values for binding of p50 to non-specific DNA were close to the calculated values (Table 1). In contrast, K_D values for binding to Ig-κB were significantly higher when calculated from the rate constants than from the Scatchard analysis (123-fold at 75 mM KCl to 4-fold at 150 mM KCl). This discrepancy could perhaps be accounted for by assuming that p50 was binding non-specifically to the flanking regions of the 30 bp DNA duplex in addition to the 10 bp binding site. In conditions of decreasing non-specific binding, i.e. increasing salt concentration, this perturbation of equilibrium binding data would be expected to become less significant, resulting in a greater similarity between calculated and measured affinities, as observed. This rationalisation is supported by the observation of biphasic dissociation from specific DNA at lower salt concentrations. Since the method for determination of k_d for Ig-κB described above involved measurements in the period of the dissociation phase once putative non-specific dissociation had diminished, this component of binding to the specific duplex was eliminated, accounting for the difference between affinities determined by Scatchard and kinetic analyses, and strongly suggesting that the calculated K_D for specific DNA is more representative of the true value than the measured value. In EMSA analyses, the presence of high concentrations of non-specific bulk carrier DNA in addition to the binding duplex eliminates this effect by competing for this non-specific component of binding. As a consequence, EMSA binding reactions must be left for significant periods of time before equilibrium binding is obtained. Inclusion of bulk carrier DNA in the SPR running buffer is not practically possible, as the binding of p50 would be obscured because the majority of the protein would be bound to the carrier DNA during the injection across the flowcell. It would also preclude analysis of binding to immobilised non-specific DNA. A reduction in the size of the flanking region of the duplex DNA was not considered suitable, since it has been suggested that p50 contacts the phosphate backbone of the DNA beyond the binding site in an uncharacterised manner (19).

DISCUSSION

We have characterised the kinetics of the interaction between NF-κB p50 and both specific and non-specific DNA under a range of salt concentrations using SPR, a technique which permits the observation of binding events in real time. Individual rate constants may thus be determined with an accuracy not possible by other techniques such as EMSA or filter-binding assays. Using this technique, we have uncovered several features of the interaction between p50 and DNA which were previously uncharacterised, and which in addition showed significant deviations from the previously reported behaviour of the *lac* repressor system.

Under buffer conditions similar to those previously reported as giving picomolar binding affinities of p50 to target DNA sequences (35), we have determined a K_D of 16 pM for the interaction of p50 with the Ig-κB binding site. This is broadly in agreement with values determined previously by equilibrium methods (11,16,35,40). However, unlike previous equilibrium studies, we have also been able to quantify the affinity of p50 to illustrative non-specific DNA under the same conditions, and we found that the K_D for this interaction was ~10 nM. Since nanomolar affinities of proteins for DNA are often associated with specific recognition events, the question of specificity is raised; the great majority of DNA sites that p50 encounters in the cell are not tight binding sequences, so a mechanism must exist to allow efficient sampling of DNA and yet allow tight binding upon sequence recognition.

It is notable that the 620-fold variation in overall affinity of p50 for specific and non-specific DNA at 100 mM KCl is manifested wholly in the different dissociation rates (Table 1). Our data suggest that the association kinetics, which at 10^6–10^7 $M^{-1}s^{-1}$ are approaching the diffusion limit, are dominated by sequence-independent long range electrostatic interactions between p50 and DNA in accord with expectation. Dissociation kinetics, however, might be expected to be strongly sequence-dependent since, whilst there is no crystal structure available for p50 complexed with non-specific DNA (or even p50 alone), it seems likely that the contribution to affinity of the specific base-contacts from the recognition loop is only maximised when a target sequence is bound. At this point the number of strong protein–DNA contacts would nearly double, and so the dissociation rate should slow down significantly, as observed.

The relatively high affinity of p50 for non-specific DNA at 100 mM KCl led us to question the physiological relevance of the data. To address this matter further, the binding kinetics were measured over a range of salt concentrations, since it is recognised that protein–DNA interactions can be sensitive to ionic strength (41). A high dependence of binding specificity on salt concentration was observed when the binding buffer was supplemented with 75–150 mM KCl. Our expectation was that

the K_D would increase with increasing salt concentration due, at least in part, to the dependence of electrostatic interactions on the inverse of the dielectric constant of the buffer, and that this drop in affinity would be manifested through both slower association rates and faster dissociation rates. However, this prediction proved to be only partially correct since the association rates actually increased slightly as the salt concentration increased (Table 1). It has previously been postulated that in DNA binding systems where the association rate constant is below the diffusion limit, a weak dependence of k_a on salt concentration is indicative of conformational changes occurring prior to binding (26). It is possible here that the changes in salt concentration subtly affect the conformation of free protein or DNA, and that this could in turn affect the association rates. Appealingly, this would be consistent with other data which strongly suggests that some structural reorganisation does indeed occur on binding of p50 to DNA (22).

When the salt dependence of the dissociation rate constants was measured, it was observed that as the salt concentration was increased from 75 to 150 mM KCl, the dissociation rate for specific DNA increased ~150-fold (Table 1). It was apparent from the data that the increase in dissociation rate with salt concentration was roughly logarithmic. This strongly suggests that the interaction between p50 and its target DNA has a highly co-operative dependence on ionic strength, consistent with the fact that the p50–DNA interaction is almost exclusively coulombic in nature (18,19). This situation is more apparent in the binding of p50 to non-specific DNA over the salt concentration range studied. From 75 to 100 mM KCl the dissociation rate for non-specific DNA increased 5.5-fold, but by 125 mM KCl no binding was detectable. Since the association rates for specific and non-specific DNA are essentially identical at the two lower salt concentrations studied, it seems reasonable to suppose that this trend continues at the higher salt concentrations and that therefore the association rate for non-specific DNA continues to increase slowly with increasing ionic strength. As no binding was observed at either 125 or 150 mM KCl, this would imply that the dissociation rate had increased greatly to effectively abolish the non-specific binding to DNA. This different and non-linear behaviour of the specific and non-specific p50–DNA complexes is in some ways reminiscent of melting of DNA duplexes of different lengths, there being a relatively sharp transition between fully bound and fully unbound in each case, but the conditions under which the transition occurs depends upon the number of co-operative interactions holding the complex together.

At this point it may be pertinent to compare these data with that from *lac* repressor–DNA binding studies. Binding of the *lac* repressor has been studied most frequently with long stretches of DNA where physiologically important processes such as sliding and interstrand transfer complicate analysis of binding kinetics (27,29). In such cases a comparison with the p50 data is difficult. However, binding of the *lac* repressor to short specific DNA sequences has been studied, and in these experiments the effects of the above processes would be minimised. In one such study (42), the *lac* repressor showed only a 1.3-fold increase in dissociation rate between 50 and 200 mM salt, whilst here p50 exhibited a 143-fold increase between 75 and 150 mM. The association rate of the *lac* repressor decreased 5–8-fold whilst that of p50 increased 3-fold across these salt concentrations. Although care should be taken when comparing data sets obtained with different protocols (notably when buffers contain mixtures of monovalent and divalent salts; 26), the magnitudes and directions of these salt effects clearly differ between the two proteins.

The data presented here also illustrate the difference between specificity and affinity of p50–DNA interactions within the salt concentration range studied. Although the absolute affinity is highest at 75 mM KCl, the K_D of 13 pM for specific DNA is at the expense of a K_D of 3.3 nM for non-specific DNA. This would likely be problematic *in vivo* since the high concentration of non-specific binding sites on chromosomal DNA would reduce the rate of specific association unless very high nuclear concentrations of p50 were present. At 125 mM KCl, however, a 6-fold weaker K_D (78 pM) for specific DNA was observed in the absence of any detectable binding to non-specific DNA, a situation which would perhaps be more appropriate for the correct functioning of a transcription factor *in vivo*. Whilst we are not claiming that our buffers are nucleoplasmic in nature, on the basis of the data presented here we do suggest that the picomolar binding affinity of p50 routinely quoted in the literature is of little physiological relevance, and that the binding we have observed at higher salt concentrations is perhaps more relevant to an *in vivo* situation. Our data seem to point to a remarkable fine-tuning of the interaction between p50 and DNA in the physiological salt concentration range, often quoted as being 140 mM K^+ or 155 mM total cation (43), to allow very rapid sampling of available sites on chromosomal DNA until a target sequence is found, at which point tight binding occurs. We have shown that even quite subtle changes in salt concentration in this range would have marked effects on this process as a result of the very strong salt dependence of the dissociation rate constants for specific and non-specific DNA. In addition, the association and dissociation rates we have measured at the higher salt concentrations suggest that NF-κB p50 may sample transcriptionally active chromosomal DNA through an efficient on–off mechanism and that a sliding mechanism may not be necessary here.

ACKNOWLEDGEMENTS

This work was supported by the BBSRC (D.J.H. and R.E.S.). R.E.S. thanks Pfizer Central Research for a BBSRC CASE studentship. M.A.C. is funded by the EPSRC and J.M.B. by a Royal Society University Research Fellowship.

REFERENCES

1 Baldwin,A.S. (1996) *Annu. Rev. Immunol.*, **14**, 649–681.
2 Ghosh,S., Gifford,A.M., Riviere,L.R., Tempst,P., Nolan,G.P. and Baltimore,D. (1990) *Cell*, **62**, 1019–1029.
3 Urban,M.B., Schreck,R. and Baeuerle,P.A. (1991) *EMBO J.*, **10**, 1817–1825.
4 Chen,F.E., Huang,D.B., Chen,Y.Q. and Ghosh,G. (1998) *Nature*, **391**, 410–413.
5 Huang,D.B., Huxford,T., Chen,Y.Q. and Ghosh,G. (1997) *Structure*, **5**, 1427–1436.
6 Nolan,G. and Baltimore,D. (1992) *Curr. Opin. Genet. Dev.*, **2**, 211–220.
7 Thanos,D. and Maniatis,T. (1995) *Cell*, **80**, 529–532.
8 Baeuerle,P. (1991) *Biochim. Biophys. Acta*, **1072**, 63–80.
9 Bushdid,P.B., Brantley,D.M., Yull,F.E., Blaeuer,G.L., Hoffman,L.H., Niswander,L. and Kerr,L.D. (1998) *Nature*, **392**, 615–618.
10 Kanegae,Y., Tavares,A.T., Izpisua Belmonte,J.C. and Verma,I.M. (1998) *Nature*, **392**, 611–614.
11 Fujita,T., Nolan,G.P., Ghosh,S. and Baltimore,D. (1992) *Genes Dev.*, **6**, 775–787.
12 Hirano,F., Tanaka,H., Hirano,Y., Hiramoto,M., Handa,H., Makino,I. and Scheidereit,C. (1998) *Mol. Cell. Biol.*, **18**, 1266–1274.

13 Paal,K., Baeuerle,P.A. and Schmitz,M.L. (1997) *Nucleic Acids Res*., **25**, 1050–1055.
14 Liou,H.-C. and Baltimore,D. (1993) *Curr. Opin. Cell. Biol*., **5**, 477–487.
15 Falvo,J.V., Thanos,D. and Maniatis,T. (1995) *Cell*, **83**, 1101–1111.
16 Thanos,D. and Maniatis,T. (1992) *Cell*, **71**, 777–789.
17 Mantovani,F., Covaceuszach,S., Rustighi,A., Sgarra,R., Heath,C., Goodwin,G.H. and Manfioletti,G. (1998) *Nucleic Acids Res.*, **26**, 1433–1439.
18 Ghosh,G., Duyne,G.V., Ghosh,S. and Sigler,P.B. (1995) *Nature*, **373**, 303–310.
19 Müller,C.W., Rey,F.A., Sodeoka,M., Verdine,G.L. and Harrison,S.C. (1995) *Nature*, **373**, 311–317.
20 Cramer,P., Larson,C.J., Verdine,G.L. and Müller,C.W. (1997) *EMBO J*., **16**, 7078–7090.
21 Chen,Y.Q., Ghosh,S. and Ghosh,G. (1998) *Nature Struct. Biol*., **5**, 67–73.
22 Matthews,J.R., Nicholson,J., Jaffray,E., Kelly,S.M., Price,N.C. and Hay,R.T. (1995) *Nucleic Acids Res*., **23**, 3393–3402.
23 Kunsch,C., Ruben,S.M. and Rosen,C.A. (1992) *Mol. Cell. Biol*., **12**, 4412–4421.
24 Barkley,M.D. (1981) *Biochemistry*, **20**, 3833–3842.
25 Barkley,M.D., Lewis,P.A. and Sullivan,G.E. (1981) *Biochemistry*, **20**, 3842–3851.
26 Record,M.T.,Jr, Ha,J.H. and Fisher,M.A. (1991) *Methods Enzymol*., **208**, 291–343.
27 Barker,A., Fickert,R., Oehler,S. and Müller-Hill,B. (1998) *J. Mol. Biol*., **278**, 549–558.
28 Levandoski,M.M., Tsodikov,O.V., Frank,D.E., Melcher,S.E., Saecker,R.M. and Record,M.T.,Jr (1996) *J. Mol. Biol*., **260**, 697–717.
29 Hsieh,M. and Brenowitz,M. (1997) *J. Biol. Chem*., **272**, 22092–22096.
30 Baeuerle,P.A. and Baichwal,V.R. (1997) *Adv. Immunol*., **65**, 111–137.
31 Lee,J.I. and Burckart,G.J. (1998) *J. Clin. Pharm*., **38**, 981–993.
32 Sodeoka,M., Larson,C., Chen,L., LeClair,K. and Verdine,G. (1993) *Biomed. Chem. Lett*., **3**, 1089–1094.
33 Gill,S.C. and von Hippel,P.H. (1989) *Anal. Biochem*., **182**, 319–326.
34 Burden,R.L. and Faires,J.D. (1993) *Numerical Analysis*. 5th Ed, PWS-Kent Publishing Compay, Boston, MA.
35 Kretzschmar,M., Meisterernst,M., Scheidereit,C., Li,G. and Roeder,R.G. (1992) *Genes Dev*., **6**, 761–744.
36 Stenberg,E., Persson,B., Roos,H. and Urbaniczky,C. (1991) *J. Colloid Interface Sci*., **143**, 513–526.
37 Myszka,D.G., Morton,T.A., Doyle,M.L. and Chaiken,I.M. (1997) *Biophys. Chem*., **64**, 127–137.
38 Karlsson,R. and Falt,A. (1997) *J. Immunol. Methods*, **200**, 121–133.
39 Bondeson,K., Karlsson,A.F., Fagerstam,L. and Magnusson,G. (1993) *Anal. Biochem*., **214**, 245–251.
40 Zabel,U., Schreck,R. and Baeuerle,P.A. (1991) *J. Biol. Chem*., **266**, 252–260.
41 Lohman,T.M. and Mascotti,D.P. (1992) *Methods Enzymol*., **212**, 400–424.
42 Goeddel,D.V., Yansura,D.G. and Caruthers,M.H. (1977) *Proc. Natl Acad. Sci. USA*, **74**, 3292–3296.
43 Alberts,B., Bray,D., Lewis,J., Raff,M., Roberts,K. and Watson,J.D. (1989) *Molecular Biology of the Cell*. Garland Publishing, Inc., New York, NY.